

## Fractal Geometry of Surface Areas of Sand Grains Probed by Pulsed Field Gradient NMR

Frank Stallmach,<sup>\*,†</sup> Corina Vogt,<sup>†</sup> Jörg Kärger,<sup>†</sup> Katrin Helbig,<sup>‡</sup> and Franz Jacobs<sup>‡</sup>

*Fakultät für Physik und Geowissenschaften, Universität Leipzig, Linnestrasse 5, 04105 Leipzig, Germany*

(Received 23 July 2001; published 25 February 2002)

Pulsed field gradient NMR self-diffusion studies of water were used to determine surface-to-volume ratios and specific surface areas of the grains forming a glacial sand deposit. Both quantities exhibit a noninteger power-law dependence as a function of the diameters of the grains. The associated fractal dimensions of the surface area ( $D_s$ ) and of the pore volume ( $D_v$ ) are found to be  $D_s - D_v = -0.70 \pm 0.05$  and  $D_s = 2.20 \pm 0.05$ . The results demonstrate that NMR studies with native pore fluids are suitable to investigate the fractal nature of natural, unconsolidated porous materials.

DOI: 10.1103/PhysRevLett.88.105505

PACS numbers: 61.43.Hv, 61.43.Gt, 76.90.+d, 91.65.-n

Fractal models for the description of porous media are discussed in basic and applied research since they offer the opportunity to characterize the structure of such heterogeneous systems by relatively simple relations over a wide range of length scales, and since they proved to be useful to predict macroscopic properties of the system studied [1–5]. In cases where geometric properties of porous systems (e.g., the pore volume, the matrix or grain volume, the specific surface area) show a power-law dependence on a characteristic length, which is determined by the measurement process or by a well-defined length in the system studied, fractal properties manifest themselves by noninteger scaling exponents connecting the characteristic lengths with the geometric properties of interest. Experimental techniques currently used to determine fractal properties of the pore geometry are based on adsorption methods [6,7], on evaluating graphical representations of the pore and matrix space obtained, e.g., from SEM images [4,8], on small-angle x-ray and neutron scattering [9–11], and on NMR microscopy [12,13], respectively. A critical review on the application of fractal models including the fractal dimensions obtained and the corresponding scaling ranges and cutoffs may be found in Refs. [2,3].

In this paper we will demonstrate that the time dependence of the self-diffusion coefficient of native fluids occupying the pore space, which is measured nondestructively by pulsed field gradient nuclear magnetic resonance (PFG NMR) [14–16], can be used to determine the fractal dimension of the surface area ( $S$ ) of unconsolidated porous media. This technique, which allows measurements of the surface-to-volume ( $S_v$ ) ratios in porous media [17–21], is combined with a method analyzing specific surface areas in dependence on the grain size originally proposed by Pfeifer and Avnir *et al.* for adsorption studies with a single type of adsorbate molecule [6,22]. In the latter method, the specific surface area  $S_m$  of a grain particle of diameter  $d_g$  and mass  $m_g$  is found to scale according to

$$S_m \equiv \frac{S}{m_g} \propto \frac{d_g^{D_s}}{d_g^3} = d_g^{D_s-3}, \quad (1)$$

where  $D_s$  denotes the fractal dimension of the surface of the grains. In Eq. (1) the volume (and hence the mass) of

the grains is assumed to scale with  $d_g^3$ . The specific surface area  $S_m$  is related to the surface-to-(pore)-volume ratio  $S_v$  by  $S_m m_g = S_v V_p$  where  $V_p$  denotes the pore volume of the porous medium. With the general assumption that the pore volume of the granulated porous medium scales with  $d_g^{D_v}$  (see, e.g., Refs. [2,8] for consolidated porous media) where  $D_v$  denotes the fractal dimension of the pore volume, the scaling behavior for the surface-to-volume ratio follows from Eq. (1):

$$S_v \equiv \frac{S}{V_p} \propto d_g^{D_s-D_v}. \quad (2)$$

For nonfractal (Euclidian) systems, the surface area  $S$  and the pore volume  $V_p$  must be proportional to  $d_g^2$  and  $d_g^3$ , respectively, which means that  $D_s = 2$  and  $D_v = 3$ . Thus,  $S_m$  and  $S_v$  in Eqs. (1) and (2) are expected to scale with  $d_g^{-1}$ . This scaling behavior can easily be proved theoretically for a random packing of monosized spherical grains.

Surface-to-volume ratios of fluid-saturated porous media may be measured by PFG NMR using the restriction of the self-diffusion at the pore/grain interface. This method analyzes the initial time dependence of the (apparent) self-diffusion coefficient  $D(\Delta)$  of the pore fluid which is controlled by the  $S_v$  ratio [17,18]

$$\frac{D(\Delta)}{D_0} = 1 - \frac{4}{9\sqrt{\pi}} S_v \sqrt{D_0 \Delta} + R(\sqrt{D_0 \Delta}). \quad (3)$$

$D_0$  denotes the self-diffusion coefficient of the pore fluid in the bulk and  $\Delta$  is the observation time over which the self-diffusion process is monitored. The value  $R(\sqrt{D_0 \Delta})$  accounts for higher order terms in  $\sqrt{D_0 \Delta}$ , which become increasingly important with increasing observation time.  $D(\Delta)$  can be studied by PFG NMR since  $\Delta$  is controlled by the time interval between the pulsed field gradients in the NMR pulse sequence. Its exact definition for restricted diffusion processes may be found in Ref. [23].

The unconsolidated sediment investigated with this approach originates from a glacial sand deposit in central Germany located about 10 km northwest of Leipzig. It was formed by the river Elster during the Elster-Saale ice age. The sand was dried on air and sieved yielding four fractions with grain diameters in the ranges of 100

to 1000  $\mu\text{m}$ . The scanning electron micrographs (SEM) of these samples presented in Fig. 1 show that the particle shapes are irregular, but there is no obvious trend that the particle shape changes with the grain size.

With respect to their bulk mineralogy and chemical surface composition analyzed by x-ray powder diffraction (XRD) and x-ray photoelectron spectroscopy (XPS), respectively, these grain size fractions are identical. They consist of quartz [(93  $\pm$  3)%] and two feldspars (microcline and albite) with a relative amount of microcline in the total feldspar fraction of 0.84  $\pm$  0.12. The averaged elemental composition of their surfaces is  $\text{Al}_1\text{Si}_{2.3}\text{O}_{9.3}\text{Fe}_{0.4}(\text{Mg}, \text{Ca})_{0.2}(\text{Na}, \text{K})_{0.1}$ . Referred to aluminum, the experimental uncertainties in the contents of the other elements detected vary between 5% for oxygen and silicon up to 40% for sodium and potassium. In all samples, oxygen, silicon, and aluminum account for (94.5  $\pm$  1.0)% of the detectable elements in the mineral surface. Additionally, their surfaces show a contamination with organic carbon [0.20  $\pm$  0.05 carbon atoms per surface (Al,Si,O) atom] resulting most likely from omnipresent microorganisms in natural sands.

From each of the grain size fractions an NMR sample was prepared by filling about 780 mg of the sand grains in a 6.5 mm inner diameter glass tube. Distilled water was added stepwise to the sands until 100% saturation of the pore space was achieved. In order to ensure a high packing density and a complete saturation of the pore space, the samples were centrifuged after each step of saturation. Finally, the samples were sealed tightly to prevent fluid loss during storage and measurement.

NMR self-diffusion measurements were carried out with a home-built NMR spectrometer FEGRIS 400 NT [24] using the 13-interval PFG NMR sequence [25] with bipolar pulsed field gradients. The high pulsed field gradient intensity ( $g_{\text{max}} = 35 \text{ T/m}$ ) available at this spectrometer allows

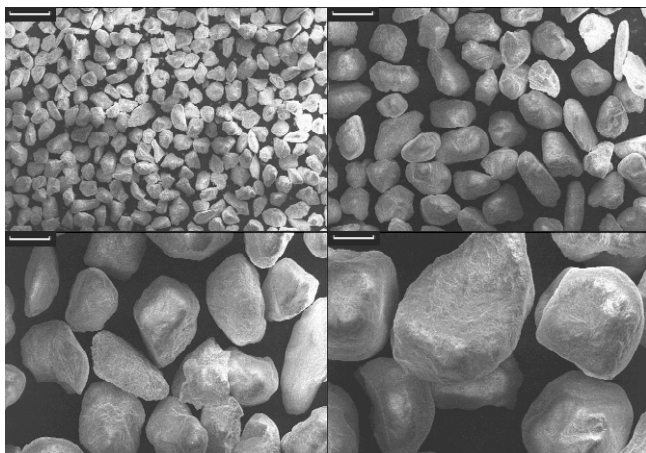


FIG. 1. SEM's of the four grain size fractions of the sand. The screen intervals used for sieving analysis are given in the legend of Fig. 2. The bars represent a length of 300  $\mu\text{m}$ .

us to perform 13-interval PFG NMR self-diffusion studies with observation times ( $\Delta$ ) as short as 2.5 ms. The timing diagram of the sequence and details of its implementation for diffusion studies in sands are given in Refs. [24,26], respectively.

By simultaneously varying the pulsed field gradient and  $\frac{\pi}{2}$  rf pulse separation in this 13-interval PFG NMR sequence [24,25], the apparent self-diffusion coefficients  $D(\Delta)$  of the water in the grain size fractions were measured in a range of  $2.5 \leq \Delta \leq 250 \text{ ms}$ . For each  $\Delta$ , the attenuation of the  $^1\text{H}$  NMR signal (spin echo) of the water was observed by successively increasing the intensity of the pulsed field gradients in 16 steps. The time dependence of the apparent self-diffusion coefficients was calculated from these sets of NMR measurements using the relations for 13-interval PFG NMR sequence given, e.g., in Refs. [23,25]. The ratios of the apparent self-diffusion coefficients to the self-diffusion coefficient in the bulk  $D(\Delta)/D_0$  are plotted in Fig. 2 as a function of  $\sqrt{D_0\Delta}$ .  $D_0$  and the  $S_v$  ratio were obtained for each grain size fraction by fitting Eq. (3) to the early time dependence of  $D(\Delta)$ . The fits are given by the solid lines in Fig. 2.

For all sands, the values of  $D_0$  obtained are in the range of  $D_0 = (2.3 \pm 0.1)10^{-9} \text{ m}^2 \text{ s}^{-1}$ , which agrees well with the known value for bulk water at the measurement temperature of 297 K. However, with decreasing grain sizes the slopes of the initial time dependencies of the apparent self-diffusion coefficients (Fig. 2) increase due to the increasing surface-to-volume ratios. In Fig. 3 the  $S_v$  ratios obtained are plotted in dependence on the grain sizes. A linear regression of  $\log S_v$  vs  $\log d_g$  yields a slope of

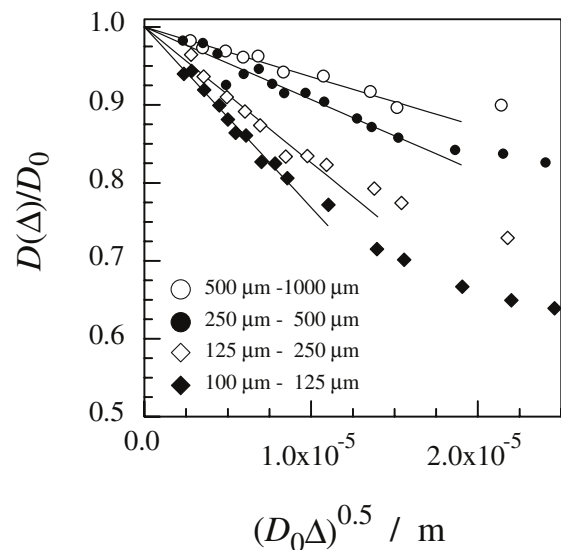


FIG. 2. Relative self-diffusion coefficients  $D(\Delta)/D_0$  as a function of  $(D_0\Delta)^{0.5}$  for water in the four grain size fractions of the sand. The solid lines represent the results of the fits of Eq. (3) to the early time dependence of these data.

$-0.70 \pm 0.05$ , which clearly deviates from  $-1$  expected for a nonfractal (Euclidian) surface and pore volume geometry.

The noninteger scaling behavior observed suggests fractal properties of the sand grains. However, possible grain size dependent artifacts of PFG NMR  $S_v$  ratio measurements caused by changes in (i) the sensitivity of the method or in (ii) molecular surface-water interaction must be excluded:

(i) The ability of PFG NMR to measure  $S_v$  ratios correctly in the range of interest is demonstrated by using beds of monosized compact spheres, which model the pore space between unconsolidated sediments. Such beds were already extensively studied [18–20]. Together with our own measurements on a random sphere pack consisting of glass spheres with a diameter of  $400 \mu\text{m}$ , their results are included in Fig. 3. The characteristic slope observed for the  $\log S_v$  vs  $\log d_g$  dependence is  $-0.92 \pm 0.05$ . It deviates only slightly from  $-1$ . Taking into account that these model systems were measured in four different laboratories representing seven different sphere packs with sphere diameters ranging from  $30$  to  $400 \mu\text{m}$ , the results for the  $S_v$  ratios must be considered to be consistent with the expected Euclidian surface and pore geometry. Thus, there is no experimental evidence for artifacts of the PFG NMR method if used to determine the scaling behavior of the  $S_v$  ratio in dependence on the grain size.

(ii) Because of the identical bulk mineralogy and chemical surface composition of the grain size fractions studied, there is no reason to assume that the averaged surface-water interactions (e.g., by hydrogen bonding) and, thus,

the surface diffusion behavior of the water changes with grain size. Moreover, since the PFG NMR  $S_v$  ratio measurements do not rely upon the surface diffusion itself but on the geometric restriction of the “free” pore water self-diffusion at the pore grain interface, they are to a large extent independent of the chemical composition of the surface [18–21].

In agreement with simple geometric considerations, Fig. 3 shows that the  $S_v$  ratio in the sands exceeds the corresponding value measured for the spheres. Moreover, the SEM images (Fig. 1) and the discussion above suggest that geometric irregularities in the surface of the grains are also responsible for the clear deviation of the slope of the  $\log S_v$  vs  $\log d_g$  plot from  $-1$ . Taking the grain size  $d_g$  obtained from sieving as the characteristic length scale and the  $S_v$  ratio measured by PFG NMR as the geometric property describing the pore space formed between the grains, it follows from the experimentally observed noninteger (fractal) scaling behavior that the surface-to-volume ratio in such sand grains is self-similar with respect to  $d_g$ . According to Eq. (2), the fractal dimensions associated with this self-similarity are  $D_s - D_v = -0.70 \pm 0.05$ .

Using only the PFG NMR results, it is not possible to decide whether the scaling behavior observed originates from fractal properties of the surface area, of the pore volume, or of both quantities. By calculating the specific surface areas  $S_m$  using the  $S_v$  ratios measured by PFG NMR and the pore volumes and the grain weights known from sample preparation, the influence of the pore volume on the surface areas measured can be separated. Figure 4 shows the resulting dependence of the specific surface areas

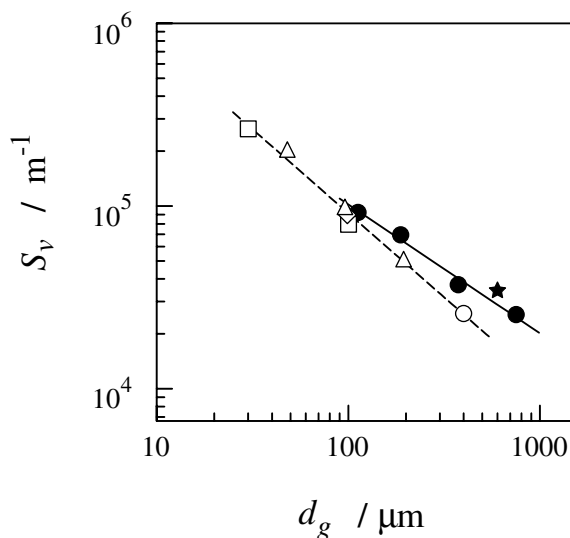


FIG. 3. Surface-to-volume ratios  $S_v$  measured by PFG NMR as a function of the grain diameters  $d_g$  for the grain size fractions ( $\bullet$ ), for the original unconsolidated sediment ( $\star$ ) and for seven different sphere packs (empty symbols:  $\circ$  this work,  $\triangle$  Ref. [18],  $\diamond$  Ref. [19],  $\square$  Ref. [20]). The full and dashed lines represent the corresponding  $\log S_v$  vs  $\log d_g$  fits.

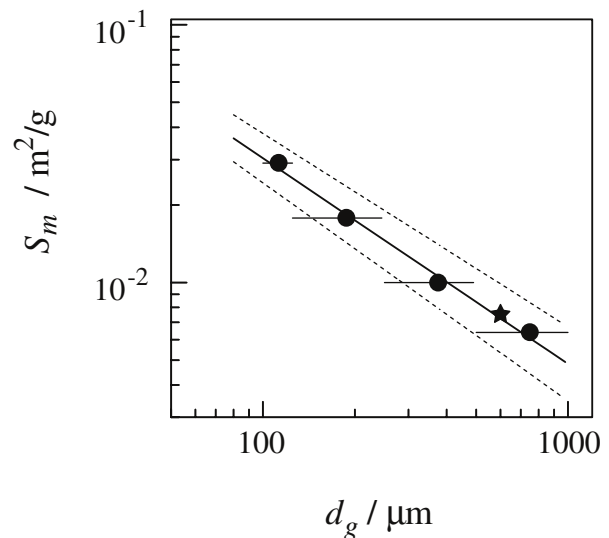


FIG. 4. Specific surface areas  $S_m$  as a function of the averaged grain diameters  $d_g$  of the grain size fractions ( $\bullet$ ) and the original sand ( $\star$ ). The full and dotted lines represent the  $\log S_m$  vs  $\log d_g$  fit and its confidence interval (see text), respectively. The horizontal error bars show the width of the screen intervals used for sieving analysis.

on the grain sizes. The  $\log S_m$  vs  $\log d_g$  fit yields a slope of  $-0.80 \pm 0.05$  clearly deviating from  $-1$ , which—according to Eq. (1)—can be attributed to a fractal dimension of the surface area of  $D_s = 2.20 \pm 0.05$ . This value is reasonable. It agrees very well with earlier results of adsorption studies on natural quartz sands which yielded fractal dimensions of  $2.21 \pm 0.01$  and  $2.15 \pm 0.05$  for Gross' quartz and Snowit, respectively (see Ref. [22] and references therein).

The length scale over which the sand grains studied exhibit surface fractal properties extends from  $d_g^{\min} \approx 100 \mu\text{m}$  up to  $d_g^{\max} \approx 1000 \mu\text{m}$ . This is small but not unusual for spatial fractals of real porous media (see Ref. [3]). Since there was no substantial amount of grains with smaller diameters, the lower cutoff is determined by the grain size distribution. The upper cutoff is given by our experimental setup which requires us to fill the unconsolidated sediments in NMR sample tubes of only 6.5 mm inner diameter. This means that beds with sand grains exceeding 1 mm in diameter cannot be reliably prepared with respect to sufficient packing density.

In PFG NMR, the mean diffusion length ( $l = \sqrt{6D_0\Delta}$ ) of the pore fluid during the shortest observation time available determines the minimum length scale by which the grain surface is probed. The applicability of Eq. (3) requires that the surface curvature radii  $r_c$  responsible for fractal properties of the grains must to be larger than this length [17]. On the other side it is reasonable to assume that  $r_c$  is smaller than the grain radius itself, leading to the inequality  $d_g/2 > r_c \geq l_{\min}$ . Using water as pore fluid ( $D_0 = 2.3 \times 10^{-9} \text{ m}^2 \text{ s}^{-1}$ ) and  $\Delta_{\min} \approx 5 \text{ ms}$ , the lower limit for detectable surface curvature radii is approximately  $10 \mu\text{m}$ . Smaller structural features on the grains are not resolved in this PFG NMR study and, thus, cannot contribute to the observed scaling law of the surface area in dependence on the grain size.

In summary, we demonstrated that investigations of surface-to-volume ratios by PFG NMR are able to reveal fractal properties of the grain surface of granulated porous media if the measurements are carried out in dependence on the grain size. The proposed approach may be a valuable addition to the experimental tools used to study properties of pore/grain interfaces, since the NMR measurements are nondestructive and since they may be performed with different liquids and gases such as, e.g., water, hydrocarbons [27], and xenon [21], respectively.

We would like to thank J. Lenzner (SEM), R. Hesse, P. Streubel (XPS), and W. Schmitz (XRD) who provided the corresponding studies of the sand, as well as P. Galvosas for his support during the NMR measurements. The authors gratefully acknowledge financial support by the German Science Foundation (SFB 294).

\*Email address: stallmac@physik.uni-leipzig.de

<sup>†</sup>Institut für Experimentelle Physik I, Universität Leipzig, Leipzig, Germany.

<sup>‡</sup>Institut für Geophysik und Geologie, Universität Leipzig, Leipzig, Germany.

- [1] *Fractals and Disordered Systems*, edited by A. Bunde and S. Havlin (Springer-Verlag, Berlin, Heidelberg, 1996).
- [2] M. Sahimi, *Flow and Transport in Porous Media and Fractured Rock* (VHC, Weinheim, 1995).
- [3] O. Malcai, D. A. Lidar, O. Biham, and D. Avnir, *Phys. Rev. E* **56**, 2817 (1997).
- [4] J. P. Hansen and A. T. Skjeltorp, *Phys. Rev. B* **38**, 2635 (1988).
- [5] H. Pape, Ch. Clauser, and J. Iffland, *Geophysics* **64**, 1447 (1999).
- [6] P. Pfeifer and D. Avnir, *J. Chem. Phys.* **79**, 3558 (1983).
- [7] S. J. Sze and T. Y. Lee, *Phys. Rev. B* **51**, 8709 (1995).
- [8] A. J. Katz and A. H. Thompson, *Phys. Rev. Lett.* **54**, 1325 (1985).
- [9] H. D. Bale and P. W. Schmidt, *Phys. Rev. Lett.* **53**, 596 (1984).
- [10] A. P. Radlinski, E. Z. Radlinska, M. Agamalian, G. D. Wignall, P. Lindner, and O. G. Randl, *Phys. Rev. Lett.* **82**, 3078 (1999).
- [11] J. Ma, H. Qi, and P. Z. Wong, *Phys. Rev. E* **59**, 2049 (1999).
- [12] H.-P. Müller, R. Kimmich, and J. Weis, *Phys. Rev. E* **54**, 5278 (1996).
- [13] A. Klemm, H.-P. Müller, and R. Kimmich, *Phys. Rev. E* **55**, 4413 (1997).
- [14] O. E. Stejeskal and J. E. Tanner, *J. Chem. Phys.* **42**, 288 (1965).
- [15] P. T. Callaghan, *Principles of Nuclear Magnetic Resonance Microscopy* (Clarendon Press, Oxford, 1991).
- [16] F. Stallmach and J. Kärger, *Adsorption* **5**, 117 (1999).
- [17] P. P. Mitra, P. N. Sen, and L. M. Schwartz, *Phys. Rev. B* **47**, 8565 (1993).
- [18] L. L. Latour, P. P. Mitra, R. L. Kleinberg, and C. H. Sotak, *J. Magn. Reson. A* **101**, 342 (1993).
- [19] G. H. Sørland, *J. Magn. Reson.* **126**, 146 (1997).
- [20] J. G. Seland, G. H. Sørland, K. Zick, and B. Hafskjold, *J. Magn. Reson.* **146**, 14 (2000).
- [21] R. W. Mair, G. P. Wong, D. Hoffmann, M. D. Hürlimann, S. Patz, L. M. Schwartz, and R. L. Walsworth, *Phys. Rev. Lett.* **83**, 3324 (1999).
- [22] D. Avnir, D. Farin, and P. Pfeifer, *J. Colloid Interface Sci.* **103**, 112 (1985).
- [23] E. J. Fordham, P. P. Mitra, and L. L. Latour, *J. Magn. Reson. A* **121**, 187 (1996).
- [24] P. Galvosas, F. Stallmach, G. Seiffert, J. Kärger, U. Kaess, and G. Majer, *J. Magn. Reson.* **151**, 260 (2001).
- [25] R. M. Cotts, M. J. R. Hoch, T. Sun, and J. T. Markert, *J. Magn. Reson.* **83**, 252 (1989).
- [26] S. Vasenkov, P. Galvosas, O. Geier, N. Nestle, F. Stallmach, and J. Kärger, *J. Magn. Reson.* **149**, 228 (2001).
- [27] F. Stallmach, C. Vogt, P. Galvosas, J. Kärger, and N. Klitzsch, *Magn. Reson. Imaging* **19**, 584 (2001).